DOI: 10.1002/adma.200801433

Continuous Size Tuning of Monodisperse ZnO Colloidal Nanocrystal Clusters by a Microwave-Polyol Process and Their Application for Humidity Sensing**

By *Xianluo Hu,* Jingming Gong, Lizhi Zhang,* and *Jimmy C. Yu**

Over the past decade, formation of monodisperse colloidal nanocrystals with size and shape control has been intensively pursued. This topic is of key importance for elucidating unique size/shape-dependent physiochemical properties and for applications in optoelectronics, sensing, catalysis, crystallization, and mineralization.[1–4] Currently, a major research direction appears to be shifting to create size and shape-selective secondary structures of colloidal nanocrystals either by self-assembly or through direct solution growth. This research trend has been evidenced by a number of interesting pioneer works published during the past several years.[5–7] As expected, manipulation of secondary structures of colloidal nanocrystals leads to fine-tuned interactions between nanocrystal subunits, and eventually enhanced collective properties and functionalities of nanocrystal ensembles.[7] In expanding fundamental exploration in this area, nevertheless, there are still concerns and challenges to chemists and materials scientists in developing efficient and cost-effective synthetic methodologies for creating secondary structures of colloidal nanocrystals. In particular, scale-up production of high-quality colloidal nanocrystals from uniform nucleation and nanocrystal growth will become critical to the realization of advanced nanodevices and many high-end nanotechnological applications. Conventional heating for producing colloidal nanocrystals, however, often relies on thermal conduction of black-body radiation to drive chemical reactions. The reaction vessel usually serves as an intermediary for energy transfer from the heating source to the solvent and finally to reactant molecules. There are inevitable disadvantages, especially at relatively low temperatures, such as sharp thermal gradients throughout the bulk solution, slow reaction kinetics, and nonuniform reaction conditions.[8] In regard to chemical scale-up, it is worth noting that inhomogeneous effects and thermal gradients would be magnified severely during nanocrystal growth. As a result, this may incur unwanted poor nucleation and/or broadened size distributions. Therefore, developing new synthetic strategies to overcome the above mentioned problems is highly desirable.

Microwave dielectric heating can address the issue of heating inhomogeneity and slow reaction kinetics. This technique is becoming an increasingly popular method of heating samples for nanomaterial synthesis. Fundamentally, microwaves heat reacting species differently than conventional means. Microwave irradiation is a clean, cheap, and convenient method of heating that often achieves higher yields and shorter reaction times.[8–10] Microwave irradiation is also unique in providing scaled-up processes without suffering from thermal gradient effects, thus opening up new avenues for potentially large-scale industrial production of high-quality nanomaterials.[11–13] More importantly, modern microwave systems possess the capabilities of time and temperature programming, allowing fast and easy optimization of experimental factors.[14] This is very beneficial for creating numerous synthetic recipes, preparing high-quality nanomaterials, and scaling up production. Recently, we have developed a microwave-enhanced hydrothermal approach for producing colloidal α-Fe_2O_3 in closed aqueous systems.[15] By controlling the reactant concentrations, we were able to achieve uniform-sized α-Fe_2O_3 nanocrystals with continuous aspect-ratio tuning and fine shape control. In this communication, a new microwave-polyol way to size-tunable ZnO nanocrystal clusters will be described.

Zinc oxide is a wide bandgap (3.37 eV) semiconductor with large exciton binding energy (60 meV). There have been many synthetic approaches reported for preparing well-defined ZnO nanostructures with diverse morphologies.[16–22] Owing to the intrinsic nature of polar hexagonal-phase ZnO with an *a*:*c* axial ratio of 1:1.6, however, most of these reported methods produce 1D or branched nanostructures. The fabrication of complex ZnO colloids with secondary microstructures is difficult because of the lack of appropriate and generalized synthetic methodologies.[21] A high-temperature nonhydrolytic sol-gel route based on the ester-elimination reaction between zinc acetate and alcohol has been proposed for growing uniform hierarchically self-assembled ZnO spheres composed of anisotropic cone-like nanocrystals as well as

[*] Dr. X. L. Hu, Prof. J. M. Gong, Prof. L. Z. Zhang
Key Laboratory of Pesticide & Chemical Biology of Ministry of Education
College of Chemistry
Central China Normal University
Wuhan 430079 (P. R. China)
E-mail: xlhu07@gmail.com
Prof. J. C. Yu, Dr. X. L. Hu
Department of Chemistry
The Chinese University of Hong Kong
Shatin, New Territories, Hong Kong (P. R. China)
E-mail: jimyu@cuhk.edu.hk

[**] The authors acknowledge the support from a Strategic Investments Scheme administrated by The Chinese University of Hong Kong and the National Science Foundation of China (grant nos. 20777026 and 20503009). Supporting Information is available online from Wiley InterScience or from the authors.

ADVANCED MATERIALS

soluble ZnO nanocrystals with tetrapod and spiked-cluster morphologies.[22a,b] Zeng and Liu fabricated three-tiered organization of ZnO nanobuilding blocks into hollow spherical conformations by a template-assisted method.[22c] More recently, aggregation of ZnO nanocrystallites involving secondary structures has been proven to be an effective way to generate light scattering within the photoelectrode film of dye-sensitized solar cells (DSSCs) while retaining the desired specific surface area for dye-molecule adsorption.[22d] Despite these advances, the assembly of ZnO colloidal nanocrystals in a facile manner into advanced secondary structures with continuous size tuning still remains a significant challenge.

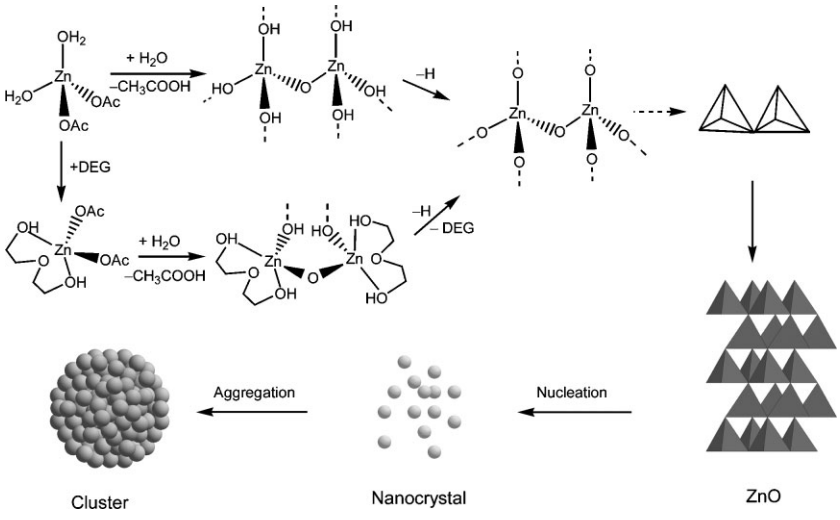

Scheme 1. Schematic representation of ZnO cluster formation. For clarity, the charges for the complexes are omitted.

Taking ZnO as an example, here we present a rapid and economical route based on an efficient microwave-polyol process to synthesize uniformly sized ZnO colloidal nanocrystal clusters (CNCs) in an open polyol system. Microwave irradiation promotes Zn(II) acetate to be hydrolyzed in diethylene glycol (DEG, a polyhydric alcohol with a boiling point of 244–245 °C) in a short time. DEG was selected as the polar solvent because of its high permittivity ($\varepsilon = 32$), enabling its high dissolving capacity for highly polar inorganic and a variety of organic compounds.[23] An additional advantage is that the high polarizability of DEG makes it an excellent microwave absorbing agent, thus leading to a high heating rate and a significantly shortened reaction time.[9] Encouragingly, this work provides the flexibility for fine tuning ZnO CNCs with precise size-control ranging from about 57 to 274 nm through an efficient and cost-effective approach that may be adopted for industrial production. To the best of our knowledge, this is the first report on the microwave-polyol synthesis of monodisperse size-tailored ZnO CNCs. The as-formed ZnO CNCs not only provide flexible building blocks for potential 3D photonic crystals, but are ideal candidates for systematically studying their nanoarchitecture-dependent performance in optical, catalytic, and sensing applications. In this work, the resulting size-tunable ZnO CNCs are used as resistor-type humidity sensors. They show quick response/recovery and high sensitivity at room temperature.

Scheme 1 illustrates the formation process of ZnO CNCs. Microwave heating at 180 °C promotes the hydrolysis of $Zn(OAc)_2$ in DEG to form zinc glycolates or alkoxide derivatives. Then, the Zn-complexes transform into ZnO nanocrystals through dehydration under microwave irradiation. This route belongs to the general *chemie douce* method and is closely related to the sol-gel process. By optimizing the experimental conditions, these fresh-formed ZnO nanocrystals spontaneously aggregate to form raspberry-like 3D clusters. Representative field-emission scanning electron microscopy (FESEM) and transmission electron microscopy (TEM) images of the products are shown in Figure 1. Clearly, the aggregates are spherical in shape and have rough surfaces. The ZnO CNCs have very narrow diameter distributions with a standard deviation of less than 5%. Close observation confirms that these monodisperse colloidal particles consist of small primary particles. We could easily tune the size of the ZnO CNCs from about 57 to 274 nm by simply decreasing the amount of Zn-complex precursors while keeping all other parameters constant. Such size tunability may arise from slight differences in the amount of H_2O and crystal nuclei induced by varying additions of Zn-complex solution. Both higher H_2O content and higher Zn-complex concentration could accelerate the hydrolysis of $Zn(OAc)_2$ and dehydration of the newly formed Zn-complexes, thus leading to more nuclei in the bulk solution and finally smaller oxide clusters. The growth of ZnO CNCs may follow the well-documented two-stage growth model,[24] whereby the primary ZnO nanocrystals (~8 nm) first nucleate in a supersaturated solution and then aggregate into larger raspberry-like assemblies (~57–274 nm in diameter). The crystalline structure of the products was characterized by X-ray diffraction (XRD). Figure 1h displays a typical XRD of the product with an average cluster diameter of 274 nm. This pattern can be indexed to a pure phase of wurtzite-type hexagonal ZnO (space group $P6_3mc$ (186), JCPDS 79-2205, $a = 3.2501$ Å, $c = 5.2071$ Å).

High-magnification TEM and high-resolution TEM (HRTEM) images provide further insight into the structural information on the secondary structure of the ZnO CNCs. Figure 2a shows a typical bright-field TEM image at a high magnification for an individual cluster of ~86 nm in diameter. Clearly, small primary nanocrystals with sizes of 6–10 nm are present in this cluster. Its corresponding electron diffraction (ED) pattern is shown in Figure 2b, suggesting the single-crystal-like nature of ZnO CNCs. Lattice fringes were recorded for a small cluster with a diameter of ~57 nm. The HRTEM image (Fig. 2c) further supports the claim of

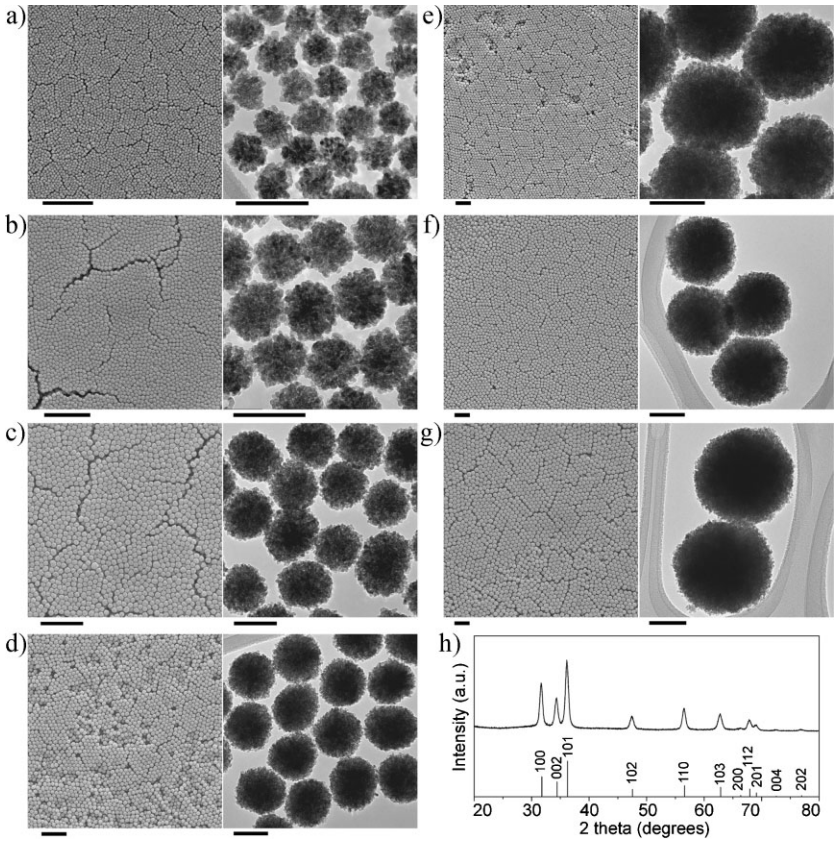

Figure 1. Representative FESEM and TEM images of ZnO CNCs. The average diameters of the CNCs, calculated by measuring more than 100 clusters for each sample, are 57 (a), 86 (b), 125 (c), 162 (d),183 (e), 210 (f), and 274 nm (g). The scale bars are 1 μm for FESEM images and 100 nm for TEM images. h) Typical XRD pattern of the 274 nm ZnO CNCs. The XRD line pattern corresponds to bulk hexagonal wurtzite ZnO (bottom).

analogous single crystallinity. As shown in Figure 2d, a representative intensity profile covers the line scan (labeled by a line in Fig. 2c) across the lattice fringes. The periodic fringe spacing of ~2.8 Å corresponds to interplanar spacing between the {100} planes of the wurtzite ZnO. Very interestingly, all of the primary nanocrystals crystallographically align with adjacent ones in the same crystal orientation. The single-crystal-like structure is also mirrored in the fast Fourier transform (FFT) pattern (inset of Fig. 2c). Nevertheless, the diffraction spots (Fig. 2b) that are slightly widened into ellipses indicate small misalignments among the primary nanocrystals. The local elemental composition of the formed clusters was confirmed by energy dispersive X-ray (EDX) microanalysis at the single-cluster level (Fig. 2e). It confirms the presence of Zn and O.

Microwave irradiation plays a crucial role in the formation of ZnO CNCs with a single-crystal-like feature based on rapid non-equilibrium kinetics. As schematically depicted in Scheme 1, small primary ZnO nuclei are generated by the rapid microwave-induced hydrolysis of Zn^{2+} and dehydration of resulting Zn-complexes in DEG at 180 °C. Meanwhile, the freshly formed nanocrystals are unstable due to their high surface energy, and thus they have a great tendency to aggregate rapidly. This aggregation process leads to final monodispersed CNCs in which the primary nanocrystals assemble through the same crystallographic orientation. Such a formation process of ZnO CNCs may be explained by the well-known growth mechanism of ''oriented attachment''.[5a,6b] Besides owing to the excellent microwave-absorbing characteristic of polar ZnO, ''hot surfaces'' on solid ZnO may be created under microwave irradiation, speeding up the nanocrystal growth and subsequent assembly into clusters. In an alternating electromagnetic field, the high conductivity and polarization of the DEG solvent and ZnO can induce localized ionic currents on the ''hot surface'' of ZnO, providing additional driving force for mass transport and directional crystallographic fusion of nanocrystals. An added benefit of the microwave field is that it can directly heat the newly formed ZnO nuclei and nanocrystals. This creates a condition where the ZnO crystals are at a substantially higher temperature than the rest of the bulk mixture. Such superheating effects cannot be achieved by conventional means.

The study of luminescence properties can shed some light on defects in the ZnO nanocrystals and their potential as photonic materials. The optical absorption spectra of the ZnO CNCs exhibit a band-edge absorption feature at about 360 nm, blue-shifted compared to that of bulk ZnO (375 nm) due to the quantum confinement effect (see Supporting Information). The room temperature photoluminescence (PL)spectra ($\lambda_{ex} = 325$ nm) of the as-formed ZnO CNCs show distinct visible emission over a wide span of wavelengths from ~450 to ~900 nm with full widths at half maximum (FWHM) of ~200 nm. However, the near bandgap exciton emission in the UV region is not obvious (see Supporting Information). The broad feature of the green-yellow emission, centered at ~584 nm, may be attributed to the presence of complex defects, e.g., singly ionized oxygen vacancies,[25a] zinc vacancies,[25b] and surface defects[25c] that are induced by rapid non-equilibrium reactions under microwave irradiation. The resulting ZnO CNCs, in spite of different sizes, exhibit similar optical absorption and photoluminescence properties, further confirming that the primary nanocrystals do not grow significantly with increasing cluster diameters.

Sensing devices based on metal oxide semiconductors play a profound role in the areas of public safety, emission control, environmental protection, and biological detection.[26] Generally, metal oxide semiconductors have excellent water-adsorbing and water-removing properties, and an electrical resistance element made of them exhibits humidity-dependent

ADVANCED MATERIALS

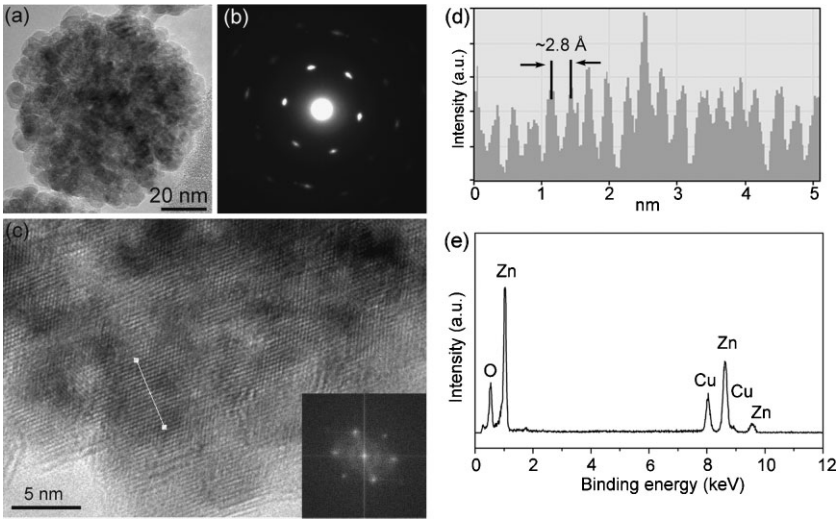

Figure 2. a) High-magnification TEM image of a single ZnO cluster of 86 nm. b) ED pattern indicating the single-crystal-like nature of the CNCs. c) Typical HRTEM image taken from a 57 nm cluster and the corresponding fast Fourier transformation (FFT) pattern (inset). d) Corresponding intensity profile for the line scan across the lattice fringes. e) EDX spectrum of a single ZnO CNC, where the signal of Cu is generated from the Cu grids.

electrical characteristics. As an n-type semiconductor, a variety of ZnO nanostructures such as nanowires and nanotetrapods have been applied in humidity sensors,[20a] and these materials indeed show a considerable increase in sensitivity as compared to their bulk counterparts. Prompted by the unique secondary and complex nanoarchitectures, we expect that the as-formed ZnO CNCs from our microwave-polyol synthesis would be advantageous for fabricating humidity sensors. A sensing unit made of ZnO CNCs for humidity sensing is shown in Scheme 2. Figure 3a shows the humidity-sensing characteristic of the thin-film sensor composed of the as-prepared ZnO CNCs of ~162 nm in diameter in response of 85% relative humidity (RH) at room temperature. The sensitivity is defined as $S = (I_h - I_a)/I_a$, where I_h is the current under a given RH and I_a is the current in dry air (5% RH). Our preliminary results show that the thin-film sensor made of ZnO CNCs exhibits high sensitivity and very good reversibility for humidity sensing. The response and recovery time are about 50 and 6 s, respectively. Such typical characteristics of the humidity sensor are ascribed to the unique nanostructure of the CNCs, which can create a film with inter-nanocrystallite and inter-cluster pores and large internal surfaces. This is significantly different from conventional film-type sensors based on compact ZnO particles. Our thin-film sensor made of monodisperse ZnO nanocrystal clusters possesses a loose-film feature analogous to a highly porous architecture and a network of interconnected hierarchical pores. The network of hierarchical inter-nanocrystallite and inter-cluster pores should contribute to the high sensitivity, since it allows the target molecules to be more accessible to all the surfaces of ZnO CNCs included in the sensing unit. This effect is similar to the already reported sensor films made of ZnO nanotetrapods,[20a] SnO_2 nanoribbons and nanowires,[27] and α-Fe_2O_3 nanorings.[15a] The most distinctive advantage of our fabrication method is that the surfaces of the produced nanocrystals remain active. Owing to the rapid non-equilibrium reactions

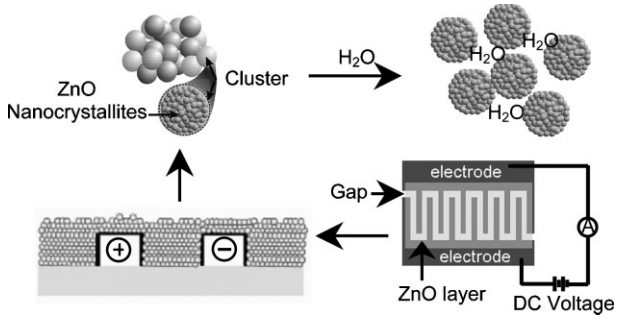

Scheme 2. Schematic illustration of the sensing unit made of ZnO CNCs.

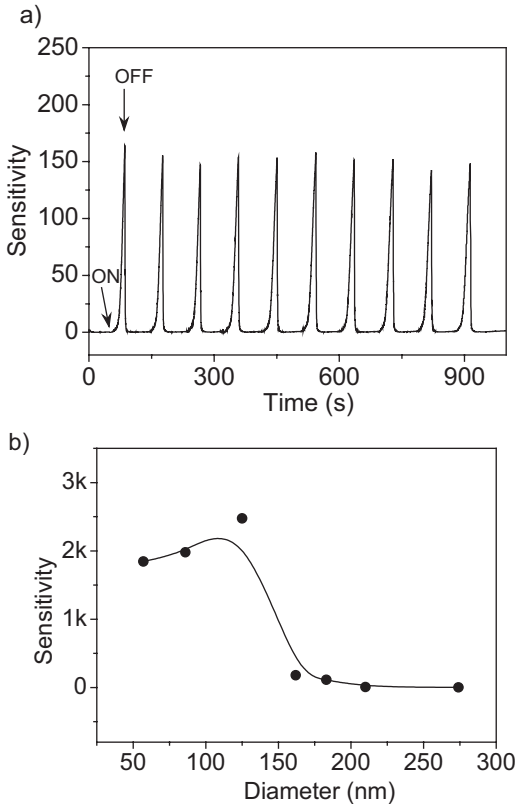

Figure 3. a) Sensitivity for a sensor made of ZnO CNCs of ~162 nm in diameter when the surrounding air was switched between water vapor-saturated (RH = 85%) and dry (RH = 5%) air at room temperature ("ON": air saturated by water vapor, "OFF": dry air). b) Sensitivity as a function of cluster diameters.

promoted by microwave irradiation, abundant oxygen vacancies exist in ZnO CNCs, as revealed by PL spectra. It is believed that our thin-film sensor for humidity detection is based on a sensing mechanism of ionic conduction. In this regard, protons dissociated from water molecules act as charge carriers that transport charge between physisorbed water molecules on the ZnO surface.[20a] Evidently, both porosity and surface activity are essential in determining the proton concentration and thus the humidity sensitivity. These are just the favorable characteristics rendered by the thin film made of ZnO CNCs. Furthermore, we have investigated the thin-film sensors made of ZnO CNCs with different diameters. The size-dependent sensitivity is shown in Figure 3b. When the diameter of the clusters is decreased from 274, to 210, to 183, to 162, to 125 nm, humidity sensitivity increases from 2.6, to 6.3, to 114, to 180, to 2476. This is easily understood because higher surface areas of smaller clusters contribute to the distinct increase in sensitivity. When further decreasing the diameter to 86 and 57 nm, however, the sensitivity would not improve but actually drops slightly. This suggests that the clusters of appropriate size between 87–125 nm possess the optimal inter-cluster porosity and internal surface area in the sensing unit, in favor of achieving high performance of ZnO CNCs for humidity sensing. It is worth noting that both high sensitivity and low operating temperature are attractive features of our sensor. We envision that the sensor can be further improved by optimizing other parameters, e.g., using more sensitive detection electronics and post-treating the ZnO CNCs through activation.

In summary, we have developed a rapid microwave-polyol process that, for the first time, offers an efficient pathway to monodisperse ZnO colloidal clusters in large quantities. The size of the clusters that are composed of small primary nanocrystals can be tuned continuously and precisely from about 57 to 274 nm by simply varying the amount of Zn- complex precursors. PL spectra indicate that the clusters composed of superfine nanocrystallites with a high surface-to-volume ratio possess a high level of surface and subsurface oxygen vacancies, resulting in a strong green-yellow emission. It is believed that the unique secondary and complex architecture of size-tunable ZnO nanocrystal clusters render them flexible building blocks for advanced functional devices. Our preliminary results demonstrate that the sensors made of ZnO CNCs exhibit high sensitivity for humidity measurement at room temperature. They should also be ideal candidates for elucidating the nanoarchitecture-dependent performance in sensing and catalytic applications, as well as in 3D photonic crystals. Compared with the existing solution-based synthetic routes that use conventional heating techniques, the present microwave-polyol approach is much more rapid, reducing the synthesis time to minutes. Also, the route for preparing tunable ZnO CNCs with narrow size distributions reported here is not only convenient but also environmentally benign and cost-effective. Therefore it is highly promising for scaled-up industrial production. Future work is underway to extend this facile microwave-polyol method to prepare metal-doped ZnO and other metal oxide CNCs with elaborate secondary structures.

Experimental

Synthesis: The ZnO CNCs were prepared in a microwave synthesis system (2.45 GHz, 300 W, Discover S-Class, CEM). The unique, circular single-mode cavity ensured that the reaction system was in a homogenous, highly dense microwave field. The system was equipped with in situ magnetic stirring, and the glass reaction flask was fit with a 15 cm air-cooled condenser. The exposure time and temperature were programmed. The automatic temperature-control system allowed continuous monitoring and control (±1 °C) of the internal temperature of the reaction systems. The preset profile (desired time and temperature) was followed automatically by continuously adjusting the applied microwave power. A $Zn(OAc)_2$/DEG stock solution was prepared by dissolving $Zn(OAc)_2 \cdot 2H_2O$ (5.4875 mg) in DEG (250 mL). In a typical synthesis, $Zn(OAc)_2$/DEG stock solution (20 mL) was microwave-treated with magnetic stirring at 180 °C for 5 min to form a slightly turbid solution and then was cooled down to room temperature, which was used as a seeding solution for further reactions. When another aliquot of the $Zn(OAc)_2$/DEG stock solution (20 mL) was microwave-heated to 120 °C within 1 min, the above-resulting seeding solution (1.8 mL) was injected rapidly into this hot mixture, and the temperature was maintained at 120 °C for 1 min. Then the reaction temperature was promptly elevated to 180 °C and further kept at this temperature for 5 min to yield 274 nm ZnO clusters. The amount of the seeding solution added determines the size of the CNCs. For example, amounts of seeding solution of 2.2, 2.5, 3, 5, 8, and 10 mL lead to ZnO CNCs with average sizes of 210, 183, 162, 125, 86, and 57 nm, respectively. The products were collected, washed with deionized water and absolute ethanol, and dried in a vacuum at 80 °C for 4 h.

Characterization: The general morphology of the products was characterized by FESEM (FEI, Quanta 400 FEG). TEM measurements were carried out on a Tecnai F20 microscope (FEI, 200 kV) and a CM 120 microscope (Philips, 120 kV) coupled with an EDX spectrometer (Oxford Instrument). XRD patterns were collected using a Bruker D8 Advance diffractometer with high-intensity Cu$K\alpha_1$ irradiation ($\lambda = 1.5406$ Å). UV-vis spectra were recorded on a UV-vis spectrophotometer (Cary 100 Scan Spectrophotometers, Varian). Room temperature PL measurements were carried out using a He/Gd laser line of 325 nm as the excitation source and a double grating monochromator connected to a photocounting system. The humidity sensors were fabricated by coating an ethanol suspension of ZnO CNCs onto alumina substrates with gold electrodes. During the measurements, the sensor was mounted in a plastic homemade chamber with a volume of 250 mL equipped with appropriate inlets and outlets for the dry and water vapor-saturated air flow.

Received: May 24, 2008
Revised: July 9, 2008
Published online: October 22, 2008

[1] a) Y. Yin, A. P. Alivisatos, *Nature* **2005**, *437*, 664; b) Y. G. Sun, Y. N. Xia, *Science* **2002**, *298*, 2176; c) X. Wang, J. Zhuang, Q. Peng, Y. D. Li, *Nature* **2005**, *437*, 121; d) Z. A. Peng, X. G. Peng, *J. Am. Chem. Soc.* **2002**, *124*, 3343; e) J. Park, K. An, Y. Hwang, J. G. Park, H. J. Noh, J. Y. Kim, J. H. Park, N. M. Hwang, T. Hyeon, *Nat. Mater.* **2004**, *3*, 891.

[2] a) X. Wang, Y. D. Li, *Chem. Commun.* **2007**, 2901; b) J. Park, J. Joo, S. G. Kwon, Y. Jang, T. Hyeon, *Angew. Chem. Int. Ed.* **2007**, *46*, 4630; c) G. Garnweitner, M. Niederberger, *J. Mater. Chem.* **2008**, *18*, 1171; d) A. R. Tao, S. Habas, P. D. Yang, *Small* **2008**, *4*, 310.

[3] a) S. R. Guo, J. Y. Gong, P. Jiang, M. Wu, Y. Lu, S. H. Yu, *Adv. Funct. Mater.* **2008**, *18*, 872; b) S. H. Im, Y. T. Lee, B. Wiley, Y. N. Xia, *Angew. Chem. Int. Ed.* **2005**, *44*, 2154; c) Y. W. Zhang, X. Sun, R. Si, L. P. You, C. H. Yan, *J. Am. Chem. Soc.* **2005**, *127*, 3260.

[4] a) L. Guo, S. H. Yang, C. L. Yang, P. Yu, J. N. Wang, W. K. Ge, G. K. L. Wong, *Appl. Phys. Lett.* **2000**, *76*, 2901; b) Y. Hu, Z. M. Jiang, C. D. Xu, T. Mei, J. Guo, T. White, *J. Phys. Chem. C* **2007**, *111*, 9757.

[5] a) J. P. Ge, Y. X. Hu, M. Biasini, W. P. Beyermann, Y. D. Yin, *Angew. Chem. Int. Ed.* **2007**, *46*, 4342; b) E. V. Shevchenko, D. V. Talapin, N. A. Kotov, S. O'Brien, C. B. Murray, *Nature* **2006**, *439*, 55.

[6] a) Y. Zhou, M. Antonietti, *J. Am. Chem. Soc.* **2003**, *125*, 14960; b) A. Narayanaswamy, H. F. Xu, N. Pradhan, X. G. Peng, *Angew. Chem. Int. Ed.* **2006**, *45*, 5361.

[7] a) J. Lee, A. O. Govorov, N. A. Kotov, *Angew. Chem. Int. Ed.* **2005**, *44*, 7439; b) L. M. Dillenback, G. P. Goodrich, C. D. Keating, *Nano Lett.* **2006**, *6*, 16; c) J. P. Ge, Y. C. Hu, Y. D. Yin, *Angew. Chem. Int. Ed.* **2007**, *46*, 7428.

[8] J. A. Gerbec, D. Magana, A. Washington, G. F. Strouse, *J. Am. Chem. Soc.* **2005**, *127*, 15791.

[9] a) S. A. Galema, *Chem. Soc. Rev.* **1997**, *26*, 233; b) M. Tsuji, M. Hashimoto, Y. Nishizawa, M. Kubokawa, T. Tsuji, *Chem. Eur. J.* **2005**, *11*, 440; c) S. Komarneni, *Curr. Sci.* **2003**, *85*, 1730; d) N. E. Leadbeater, *Chem. Commun.* **2005**, 2881.

[10] a) Y. J. Zhu, W. W. Wang, R. J. Qi, X. L. Hu, *Angew. Chem. Int. Ed.* **2004**, *43*, 1410; b) X. L. Hu, Y. J. Zhu, S. W. Wang, *Mater. Chem. Phys.* **2004**, *88*, 421; c) Y. J. Zhu, X. L. Hu, *Chem. Lett.* **2003**, 1140.

[11] a) I. Bilecka, I. Djerdj, M. Niederberger, *Chem. Commun.* **2008**, 886; b) Q. Y. Lu, F. Gao, S. Komarneni, *J. Mater. Res.* **2004**, *19*, 1649; c) Q. Y. Lu, F. Gao, S. Komarneni, *J. Am. Chem. Soc.* **2004**, *126*, 54.

[12] a) S. Makhluf, R. Dror, Y. Nitzan, Y. Abramovich, R. Jelinek, A. Gedanken, *Adv. Funct. Mater.* **2005**, *15*, 1708; b) S. Bhattacharyya, A. Gedanken, *J. Phys. Chem. C* **2008**, *112*, 659.

[13] a) A. B. Panda, G. Glaspell, M. S. El-Shall, *J. Am. Chem. Soc.* **2006**, *128*, 2790; b) A. B. Panda, G. Glaspell, M. S. EI-Shall, *J. Phys. Chem.* **2007**, *111*, 1861; c) G. Buehler, C. Feldmann, *Angew. Chem. Int. Ed.* **2006**, *45*, 4864.

[14] a) E. B. Celer, M. Jaroniec, *J. Am. Chem. Soc.* **2006**, *128*, 14408; b) J. C. Yu, X. L. Hu, Q. Li, Z. Zheng, Y. M. Xu, *Chem. Eur. J.* **2006**, *12*, 548; c) X. L. Hu, J. C. Yu, *Chem. Asian J.* **2006**, *1*, 605; d) J. C. Yu, X. L. Hu, Q. Li, L. Z. Zhang, *Chem. Commun.* **2005**, 2704; e) X. L. Hu, J. C. Yu, J. M. Gong, Q. Li, *Cryst. Growth Des.* **2007**, *7*, 2444.

[15] a) X. L. Hu, J. C. Yu, J. M. Gong, Q. Li, G. S. Li, *Adv. Mater.* **2007**, *19*, 2324; b) X. L. Hu, J. C. Yu, *Adv. Funct. Mater.* **2008**, *18*, 880; c) X. L. Hu, J. C. Yu, J. M. Gong, *J. Phys. Chem. C* **2007**, *111*, 11180.

[16] a) M. H. Huang, S. Mao, H. Feick, H. Q. Yan, Y. Y. Wu, H. Kind, E. Weberm, R. Russo, P. D. Yang, *Science* **2001**, *292*, 1897; b) Z. L. Wang, J. H. Song, *Science* **2006**, *312*, 242; c) F. Li, Y. Ding, P. X. Gao, X. Q. Xin, Z. L. Wang, *Angew. Chem. Int. Ed.* **2004**, *43*, 5328.

[17] a) N. Pinna, G. Garnweitner, M. Antonietti, M. Niederberger, *J. Am. Chem. Soc.* **2005**, *127*, 5608; b) L. Vassieres, *Adv. Mater.* **2003**, *15*, 646; c) S. H. Yu, H. Cölfen, *J. Mater. Chem.* **2004**, *14*, 2124.

[18] a) R. Q. Song, A. W. Xu, B. Deng, Q. Li, G. Y. Chen, *Adv. Funct. Mater.* **2007**, *17*, 296; b) Y. Peng, A. W. Xu, B. Deng, M. Antonietti, H. Colfen, *J. Phys. Chem. B* **2006**, *110*, 2988; c) W. W. Wang, Y. J. Zhu, L. X. Yang, *Adv. Funct. Mater.* **2007**, *17*, 59.

[19] a) M. S. Mo, S. H. Lim, Y. W. Mai, R. K. Zheng, S. P. Ringer, *Adv. Mater.* **2008**, *20*, 339; b) M. S. Mo, J. C. Yu, L. Z. Zhang, S. K. A. Li, *Adv. Mater.* **2005**, *17*, 756.

[20] a) Y. F. Qiu, S. H. Yang, *Adv. Funct. Mater.* **2007**, *17*, 1345; b) B. Liu, H. C. Zeng, *J. Am. Chem. Soc.* **2004**, *126*, 16744; c) G. Z. Shen, Y. Bando, B. D. Liu, D. Golberg, C. J. Lee, *Adv. Funct. Mater.* **2006**, *16*, 410.

[21] a) D. Jezequel, J. Guenot, N. Jouini, F. Fievet, *J. Mater. Res.* **1995**, *10*, 77; b) E. W. Seelig, B. Tang, A. Yamilov, H. Cao, R. P. H. Chang, *Mater. Chem. Phys.* **2003**, *80*, 257; c) H. M. Cheng, H. C. Hsua, S. L. Chen, W. T. Wu, C. C. Kao, L. J. Lin, W. F. Hsieh, *J. Cryst. Growth* **2005**, *277*, 292.

[22] a) J. Joo, S. G. Kwon, J. H. Yu, T. Hyeon, *Adv. Mater.* **2005**, *17*, 1873; b) X. H. Zhang, Y. Y. Feng, Y. L. Zhang, I. Lieberwirth, W. Knoll, *Small* **2007**, *3*, 1194; c) B. Liu, H. C. Zeng, *Chem. Mater.* **2007**, *19*, 5824; d) Q. F. Zhang, T. P. Chou, B. Russo, S. A. Jenekhe, G. Z. Cao, *Angew. Chem. Int. Ed.* **2008**, *47*, 2436.

[23] a) C. Feldmann, *Adv. Mater.* **2001**, *13*, 1301; b) C. Feldmann, H. O. Jungk, *Angew. Chem. Int. Ed.* **2001**, *40*, 359; c) C. Feldmann, *Adv. Funct. Mater.* **2003**, *13*, 101.

[24] S. Libert, V. Gorshkov, D. Goia, E. Matijeviæ, V. Privman, *Langmuir* **2003**, *19*, 10679.

[25] a) K. Vanheusden, W. L. Warren, C. H. Seager, D. R. Tallant, J. A. Voigt, B. E. Gnade, *J. Appl. Phys.* **1996**, *79*, 7983; b) Y. W. Heo, D. P. Norton, S. J. Pearton, *J. Appl. Phys.* **2005**, *98*, 073502; c) N. E. Hsu, W. K. Hung, Y. F. Chen, *J. Appl. Phys.* **2004**, *96*, 4671.

[26] a) N. Pinna, G. Neri, M. Antonietti, M. Niederberger, *Angew. Chem. Int. Ed.* **2004**, *43*, 4345; b) J. Polleux, A. Gurlo, N. Barsan, U. Weimar, M. Antonietti, M. Niederberger, *Angew. Chem. Int. Ed.* **2006**, *45*, 261.

[27] Y. L. Wang, X. C. Jiang, Y. N. Xia, *J. Am. Chem. Soc.* **2003**, *125*, 16176.